

Transient response analysis for temperature-modulated chemoresistors

R. Gutierrez-Osuna^{a,*}, A. Gutierrez-Galvez^a, N. Powar^b

^aDepartment of Computer Science, Texas A&M University, College Station, TX 77843-3112, USA

^bDepartment of Computer Science and Engineering, Wright State University, Dayton, OH 45435, USA

Abstract

This article presents a sensor excitation and signal processing approach that combines temperature modulation and transient analysis to enhance the selectivity and sensitivity of metal-oxide gas sensors. A staircase waveform is applied to the sensor heater to extract transient information from multiple operating temperatures. Four different transient analysis techniques, Pade–Z-transform, multi-exponential transient spectroscopy (METS), window time slicing (WTS) and a novel ridge regression solution, are evaluated on the basis of their ability to improve the sensitivity and selectivity of the sensor array. The techniques are validated on two experimental databases containing serial dilutions and mixtures of organic solvents. Our results indicate that processing of the thermal transients significantly improves the sensitivity of metal-oxide chemoresistors when compared to the quasi-stationary temperature-modulated responses.

© 2003 Elsevier Science B.V. All rights reserved.

Keywords: Transient response analysis; Pattern recognition; Gas sensor arrays; Electronic nose; Multi-exponential models; Temperature modulation

1. Introduction

The temperature-selectivity dependence of metal-oxide semiconductor (MOS) materials can be exploited to improve the information content of chemoresistors by modulating the operating temperature of the device during exposure to analytes and processing the resulting dynamic response [1]. Temperature modulation approaches for MOS sensors can be broadly classified into two categories: temperature cycling and thermal transients. In temperature cycling (TC), the sensor is excited with a periodic heater voltage, typically a sinusoidal waveform to ensure a smooth temperature profile. To help resolve the various peaks in sensitivity that may occur during the cycle, a slow varying sine wave is often desirable [2]. If the heater waveform is slow enough to allow the sensor to approach the set-point temperature, the behavior of the sensor at each temperature may then be treated as a “pseudo-sensor” by virtue of the relationship between operating temperature and sensor selectivity. In thermal transients (TT), on the other hand, the sensor is driven by a step or pulse waveform in the heater voltage, and the discriminatory information is contained in the chemical transient induced by the fast change in temperature.

To the best of our knowledge, the work of Sears et al. [3,4] constitutes one of the first studies on temperature cycling for metal-oxide sensors. The authors used a Figaro sensor with a sinusoidal heater voltage, and analyzed selectivity and sensitivity as a function of the frequency and the heater voltage for different analyte concentrations. For more than a decade, Nakata and co-workers [5–9] have also used a sinusoidal heater voltage for temperature modulation purposes. The authors transform the sensor response into the frequency domain by means of the fast Fourier transform (FFT), and use the coefficients of higher harmonics to discriminate various analytes [6–9]. Nakata et al. [7], and Nakata and Yoshikawa [8] have also applied these procedures to qualitatively characterize the mixtures of two gases. However, no quantitative classification was performed. Heilig et al. [10] have used multi-layer perceptrons (MLPs) to process the FFT features of the sensor response to a sinusoidal temperature modulation. The authors utilize two separate MLPs to perform a quantitative and qualitative analysis of the gases. The MLPs are able to detect the presence of an analyte in a mixture and predict the concentration of a single gas and gas mixtures. Llobet et al. [11] have applied the discrete wavelet transform to extract features that are more informative than those provided by the FFT. The authors have used two different neural networks, fuzzy ARTMAP and MLPs, coupled with leave-one-out and bootstrap for validation purposes. Perez-Lisboa et al. [12]

* Corresponding author. Tel.: +1-979-845-2942; fax: +1-979-847-8578.
E-mail address: rgutier@cs.tamu.edu (R. Gutierrez-Osuna).

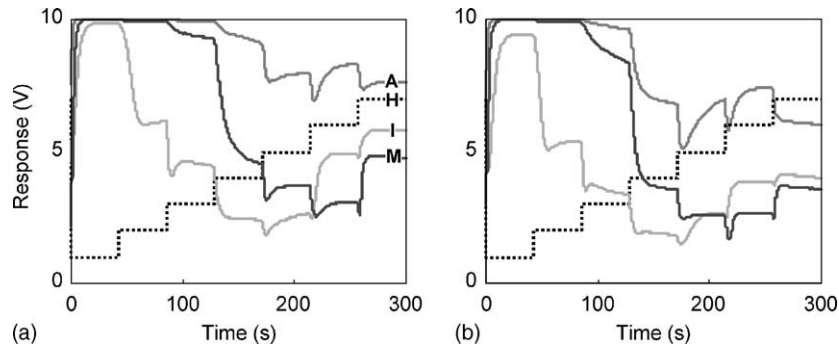


Fig. 1. Staircase thermal modulation for two MOS sensors: (a) TGS2600; (b) TGS2620. H, heater voltage; A, acetone; I, isopropyl alcohol; M, ammonia.

have used the dc and ac RMS values from the sensor response to a periodic excitation signal. Wlodek et al. [13] have used a ramp as a heater excitation signal. The response of the sensor is modeled with a family of Gaussian curves and the parameters of the curves are used as features. Using micro-hotplate sensors, Kunt and co-workers [14,15] have developed a numerical optimization procedure capable of deriving a temperature profile that maximizes the discrimination between two analytes of interest.

In the realm of temperature modulation with transients, Hiranaka et al. [16] have analyzed the cooling temperature transients when the heater supply is switched from a high voltage to a low voltage. The response of the sensor for different odors presents peaks at different positions in the transient. Similar results have also been achieved by Amamoto et al. [17]. Kato et al. [18] have used a pulse signal to drive the heater voltage. A phenomenological equation with four parameters is used to model the sensor response to each analyte and the model parameters are used as features. Yea et al. [19] have used a train of pulses to discriminate and quantify flammable gases. The authors process the sensor response with the FFT, and the ac components are passed to an MLP to determine which odor is present. Once the odor has been recognized, the output of the MLP, along with the dc component of the FFT, is passed to a neuro-fuzzy algorithm to estimate the concentration.

This article describes a sensor excitation technique that combines characteristics from the two above-mentioned temperature modulation approaches. The technique, termed staircase thermal modulation (STM), drives the sensor heater with a voltage that consists of a series of step inputs at different voltage levels, forming a staircase waveform, as shown in Fig. 1 for two Figaro sensors [20]. Each step in temperature yields a thermal transient with a characteristic shape that depends not only on the voltage range but also on the particular analyte to which the sensor is being exposed. Computational transient analysis [21] of each step response is then employed to extract additional information from the sensor. In particular, this article explores four unique transient analysis techniques as potential feature extraction tools for thermal transients: the Pade-Z-transform [22], multi-exponential transient spectroscopy (METS) [23], window

time slicing (WTS) [24] and a novel ridge regression curve fitting (RRCF) technique. These four techniques are compared with the steady-state response of the sensor at each temperature level, which serves as a baseline technique for temperature-modulated sensors.

2. Transient response analysis

Our prior work on transient analysis for chemical sensors has focused on the dynamic response of the sensor when exposed to a step function in the concentration of an analyte. As presented in [21], chemical transients can be accurately modeled by a set of real exponentials:

$$f(t) = \sum_{m=1}^M G_m e^{-t/\tau_m}, \quad (1)$$

where G_m and τ_m are the amplitude and time constant of the m th exponential decay. This parametric representation of the sensor transient serves two distinct purposes. First, a compact representation of the sampled data $\{f_k; k = 0, \dots, N-1\} \rightarrow \{G_m, \tau_m; m = 1, \dots, M\}$ is obtained. Second, the family of time constants and amplitudes $\{G_m, \tau_m; m = 1, \dots, M\}$ can be used as a feature vector for pattern recognition purposes. Although conceptually straightforward, the task of modeling a curve with a set of exponential functions with real exponents is ill conditioned. Unlike the familiar sinusoidal functions used in Fourier analysis, exponential decays do not constitute an orthogonal base. Therefore, if one tries to determine the coefficients $\{G_m, \tau_m; m = 1, \dots, M\}$ from finite-time and finite-precision samples of the transient, the distribution function of time constants will not be unique. An additional problem is the determination of M , the number of exponential components that should be used in the fit. These issues have been known for over 40 years, when Lanczos demonstrated that three exponential curves with similar time constants could be fitted accurately with two exponential models with significantly different amplitudes and time constants [25]. A number of methods to find real exponential components from experimental data have been proposed in the literature.

In an earlier article [21], we have performed a thorough literature review of these methods and concluded that the Pade–Z-transform was the most appropriate method for the problem of gas sensor modeling.

An alternative model to the finite set of exponential decays in (1) is to compute a continuous distribution of time constants, which may be considered as a spectral representation of the transient signal:

$$F(t) = \int_0^{\infty} G(\tau) e^{-t/\tau} d\tau. \quad (2)$$

To the best of our knowledge, only two such spectral techniques have been used to process transient signals: METS [23] and the Gardner transform [26]. METS has been shown [23] to be suitable for processing chemical transients in gas sensors and is, for this reason, selected for our study.

In Sections 2.1–2.4, we present a brief overview of the Pade–Z-transform, METS and ridge regression curve fitting. The latter may be considered a hybrid technique in that it uses the model in (1) to produce a spectral representation of a transient signal.

2.1. The Pade–Z procedure

The Pade–Z-transform is based on the theory of Pade approximants and the Z-transform of discrete systems. The Pade–Z-transform has had an interesting history: although the term was coined by Yeramian and Claverie in 1987, it has been known for over 200 years. Its original ancestor is the Prony’s method, which was reformulated using the Z-transform by Weiss and McDonough in 1963 [27]. The Pade–Z method is derived as the discrete-time version of the Pade–Laplace method of Yeramian and Claverie [22], which uses the Laplace transform of continuous systems. The Pade–Z-transform has been shown to be more appropriate for time series with a few samples and, unlike the Pade–Laplace method, does not suffer from numerical integration problems.

The goal of the Pade–Z procedure is to obtain the parametric model of Eq. (1) from a sampled transient $\{f_k; k = 0, \dots, N-1\}$. One may be initially tempted to find the model parameters through the least squares solution:

$$\{M, G_m, \tau_m\} = \arg \min_{M, G_m, \tau_m} \left[\sum_{k=0}^{N-1} \left(f_k - \sum_{m=1}^M G_m e^{-kT/\tau_m} \right)^2 \right]. \quad (3)$$

However, (3) yields a non-linear system of equations in the parameters τ_m , requires knowledge of the number of components M and is known to be numerically ill conditioned. To avoid these problems the Pade–Z-transform operates in the discrete Z-domain [28]. The one-sided Z-transform of $\{f_k; k = 0, \dots, N-1\}$ is:

$$F_1(z) = Z[f_k] = \sum_{k=0}^{N-1} f_k z^{-k}, \quad (4)$$

whereas the closed-form Z-transform of (1) is:

$$F_2(z) = Z[f_k] = \sum_{m=1}^M G_m \frac{z}{z - e^{-T/\tau_m}}. \quad (5)$$

Estimation of the parameters $\{G_m, \tau_m; m = 1, \dots, M\}$ is then accomplished by expressing the series $F_1(z)$ in the same closed form as $F_2(z)$. A Pade approximant is used to represent the series $F_1(z)$ as a rational expression $R(z) = N(z)/D(z)$. From this expression, $F_2(z)$ can be obtained by performing a partial-fraction expansion. This technique is known as Prony’s method. The Pade–Z-transform is a generalization of Prony’s method. Instead of using $F_1(z)$ as the Z-transform of the time series, the Pade–Z method uses its Taylor series expansion $\hat{F}_1(\xi) = \sum_{j=0}^{\infty} c_j (\xi - \xi_0)^j$ at a point $z_0 = 1/\xi_0$ [22]. Prony’s method then becomes the particular case of the Pade–Z method for $z_0 = +\infty$. Experience shows that there exists an optimal range of values of z_0 for the detection of exponential components, which does not contain the values 0 or ∞ . This fine-tuning parameter greatly enhances the resolution capabilities of the Pade–Z method and explains the unsatisfactory behavior of the standard Prony’s method [22]. Due to space constraints, the reader is referred to [21,29] for additional details of the Pade–Z method for modeling gas sensor transients.

2.2. Multi-exponential transient spectroscopy

In analogy to the Fourier transform, which extracts the frequency content of a stationary signal, there also exist spectral techniques that estimate the distribution of time constants in a transient signal. In particular, the METS method of Marco et al. [23] has been shown to be suitable for processing chemical transients in gas sensors. METS is based on a multiple differentiation of the signal transient (1) in logarithmic-time scale $y = \ln(t)$:

$$\text{METS}_1(t) = \frac{d(f(t))}{d(\ln t)} = \sum_{m=1}^M G_m h(y - \ln \tau_m). \quad (6)$$

This signal, known as the first-order METS signal, is the convolution of the ideal time-constant distribution $G(\tau) = \sum_{m=1}^M G_m \delta(\tau - \tau_m)$, where the Dirac delta function $\delta(\cdot)$ is replaced with an asymmetric kernel function $h(y) = \exp(y - \exp(y))$. To facilitate the differentiation in (6), the signal transient needs to be sampled at geometrically spaced times $t = t_0 q^p$ with $q > 1$. In our case, this is accomplished by spline interpolation from a uniformly sampled sensor transient $f_k = f(kT)$. METS_1 can then be obtained using a Lagrange differentiator [23], yielding:

$$\text{METS}_1(p) = 2 \left(\frac{f(t_0 q^{p+m}) - f(t_0 q^{p-m})}{3m \ln q} \right) - \frac{f(t_0 q^{p+2m}) - f(t_0 q^{p-2m})}{12m \ln q}. \quad (7)$$

In the present implementation, values of $m = 3$ and $q = 2^{1/3}$ were used. Improved time-constant resolution can be obtained, at the expense of amplifying high-frequency noise, by subsequent differentiation of the convolution product, yielding higher-order signals $METS_n$, which can be interpreted as the convolution of $G(\tau)$ with narrower kernels $h_n(y) = \exp(ny - \exp(y))$:

$$METS_1(t) = \sum_{m=1}^M G_m h_n(y - \ln \tau_m). \tag{8}$$

These higher-order METS signals can be conveniently obtained in a recursive fashion by:

$$METS_{n+1}(p) = nMETS_n(p) - \frac{METS_n(p) - METS_n(p-1)}{\ln q}. \tag{9}$$

Due to the wide dynamic range in resistances for temperature-modulated MOS sensors, the sampled transients are subject to quantization noise, preventing us from using higher-order METS signals. Thus, our study will be limited to the first spectrum, $METS_1$.

2.3. Ridge regression curve fitting

As stated earlier, direct minimization of the objective function (3) is impractical, primarily as a result of the non-linearity introduced by the time constants. If the correct time constants are known, though, the amplitudes G_m can in principle be obtained from the linear least-squares solution of (3) by means of the following system of equations:

$$\begin{bmatrix} e^{-T/\tau_1} & e^{-T/\tau_2} & \dots & e^{-T/\tau_m} \\ e^{-2T/\tau_1} & e^{-2T/\tau_2} & & e^{-2T/\tau_m} \\ & & \ddots & \vdots \\ e^{-NT/\tau_1} & e^{-NT/\tau_2} & \dots & e^{-NT/\tau_m} \end{bmatrix} \begin{bmatrix} G_1 \\ G_2 \\ \vdots \\ G_m \end{bmatrix} = \begin{bmatrix} f_1 \\ f_2 \\ \vdots \\ f_N \end{bmatrix}, \tag{10}$$

or in matrix notation, $EG = F$, with the pseudo-inverse solution defined by:

$$G = [E^T E]^{-1} E^T F = E^\dagger F. \tag{11}$$

This direct solution requires a further refinement since the regression matrix E is highly co-linear. To stabilize this

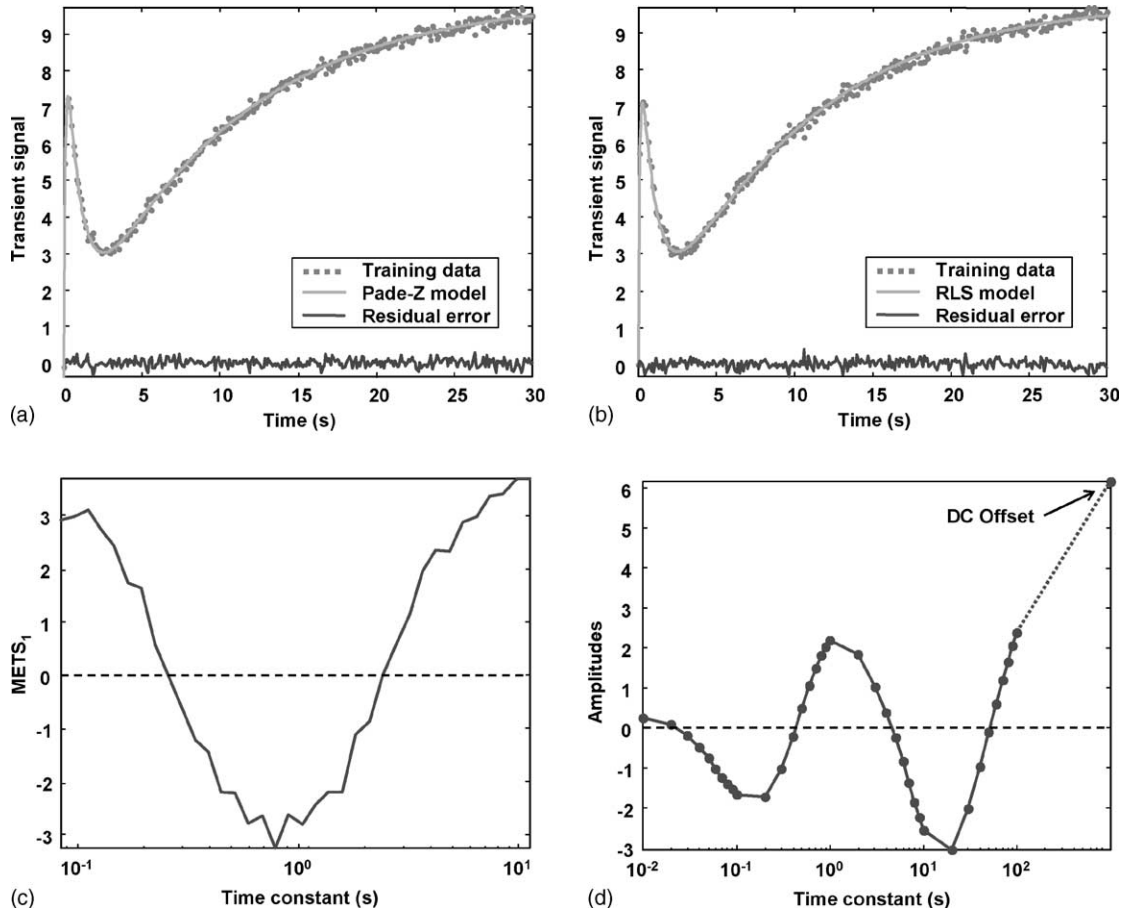


Fig. 2. Curve fit provided by: (a) Pade-Z; (b) ridge regression. Time-constant spectra generated by: (c) METS; (d) ridge regression.

least-squares solution, we regularize the covariance matrix $E^T E$ by adding a multiple of the identity matrix:

$$G = \left[(1 - \gamma) E^T E + \gamma \frac{\text{tr}(E^T E)}{M} I \right]^{-1} E^T F, \quad (12)$$

where γ ($0 \leq \gamma \leq 1$) is a regularization parameter [30] that controls the amount of shrinkage toward the identity matrix. This solution is known as ridge regression (RR) in the statistics and neural network community. Notice that the RR solution still requires knowledge of the time constants τ_m . These may be found by computing (12) for different subsets of time constants and selecting the subset with lowest mean-squared-error, an approach that appears to be rather computationally involved. Instead, we employ a fine-grained set of time constants in logarithmic scale $\tau = \{0.01, 0.02, \dots, 0.09, 0.1, 0.2, \dots, 0.9, 1, 2, \dots, 9, \dots\}$, which provides a distribution of amplitudes that may also be treated as a spectral representation of the transient. A dc term is also included to absorb the steady-state response of the sensor.

2.4. Validation of the proposed techniques

To illustrate the capabilities of the three proposed techniques, we utilize a synthetic transient signal containing three exponential decays. The exponentials have amplitudes ($G_1 = -10$, $G_2 = +10$, and $G_3 = -10$) and time constants one decade apart ($\tau_1 = 0.1$ s, $\tau_2 = 1$ s, and $\tau_3 = 10$ s). To make the problem more interesting, a dc offset $G_0 = 10$ and Gaussian noise $N(\mu = 0, \sigma = 0.1)$ are added to the signal. The transient is simulated with a sampling rate $T = 1/100$ s from $t = 0$ until $t = 100$ s to allow for the exponential to die out.

Pade-Z returns a model containing three exponential components with amplitudes ($G_1 = -9.8534$, $G_2 = 10.0663$, and $G_3 = -10.0803$) and time constants ($\tau_1 = 0.1010$ s, $\tau_2 = 1.0190$ s, and $\tau_3 = 9.7878$ s), but only after the final value of the transient $f(t = 100$ s) is subtracted from the transient. Otherwise, Pade-Z tends to return an additional exponential with a very large and unstable time constant to absorb the non-zero steady state caused by the dc offset. Fig. 2(a) illustrates the accuracy of the curve fit provided by the Pade-Z-transform.

The METS signal, shown in Fig. 2(c), presents three clear peaks at 10^{-1} , 1 and 10 s but is not able to capture the steady-state component of the signal. The curve fit and spectrum returned by the RRCF signal are shown in Fig. 2(b) and (d), respectively. RRCF is able to provide an accurate curve fit and, additionally, a distribution of amplitudes that can be interpreted as a spectrum. Notice how RRCF can also capture the steady state of the signal, both by means of the dc offset and the amplitude of the larger time constants.

3. Feature extraction

The three techniques presented in Section 2 provide a transformation from the time domain onto the “time-constant” domain where information in the sensor transients may be enhanced. A number of approaches have also been explored to extract information directly from the time domain. Some of these methods compute descriptive parameters such as rise times, maximum/minimum responses and slopes, curve integrals, etc., whereas other approaches subsample the sensor response at different times during the transient [31]. For the purpose of comparing the relative merits of time and time-constant domain representations, this article will also consider WTS [24], a subsampling technique that employs a family of bell-shaped kernels to integrate the transient response at different time windows. The advantage of WTS over parametric features (e.g. rise time) is that it can also be employed as a filter bank to extract information from spectral representations, as illustrated in Fig. 3(b). Feature extraction from the Pade-Z model requires a closer consideration, and is covered next.

Ideally the Pade-Z parameters $\{G_m, \tau_m\}$ could be used directly as input features into a pattern classifier. To illustrate the discriminatory capabilities of these parameters, Fig. 4 presents a scatter plot of the time constants and amplitudes returned by the Pade-Z-transform for a particular sensor and thermal transient. Notice how the model produces three exponential decays for each of four samples of acetone (A) and isopropyl alcohol (I) but only one for ammonia (M). This ability of the Pade-Z procedure to automatically

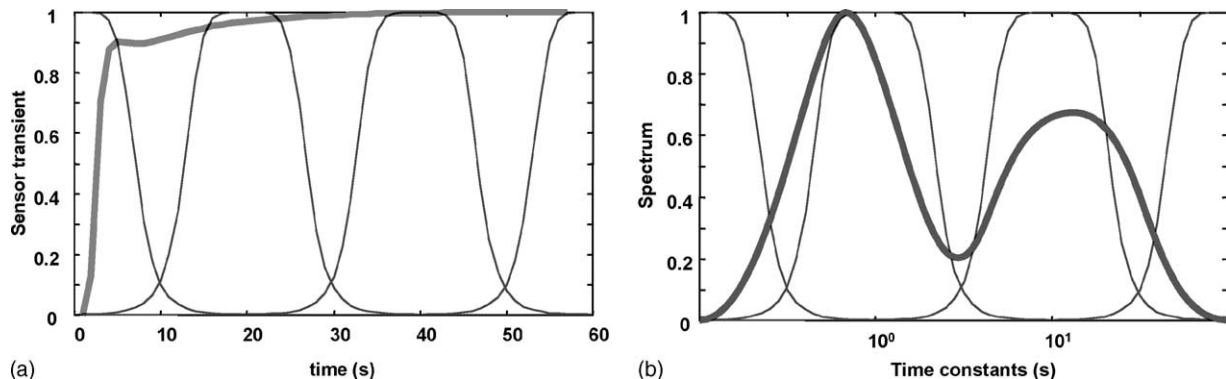


Fig. 3. Window time slicing from: (a) temporal representation; (b) spectrum of time constants.

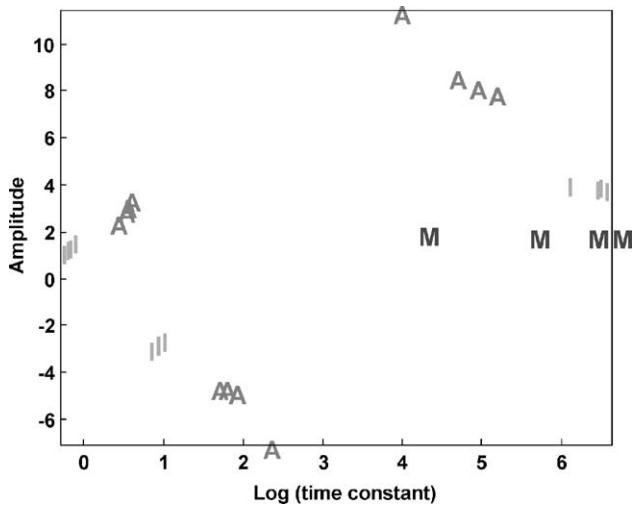


Fig. 4. Time constants and amplitudes extracted by Pade–Z from a 5–6 V thermal transient of a TGS2620 sensor. A, 10^{-4} vol.% acetone; I, 10^{-1} vol.% isopropyl alcohol; M, 1 vol.% ammonia. Four samples of each analyte were extracted.

select an appropriate number of exponential decays introduces a complication if these model parameters are to be used directly as features, since many pattern-classification algorithms expect a fixed-size feature vector. This issue can be addressed in a number of ways. First, a constant feature vector with the maximum number of exponential components $\{G_m, \tau_m; m = 1, \dots, M_{\max}\}$ could be used. For each transient, and depending on the number of components returned by the Pade–Z, several of the $\{G_m, \tau_m\}$ pairs would be padded with zeros. This naïve approach, however, does not account for the fact that the Pade–Z procedure can (and oftentimes does) return solutions with different number of exponentials for two transients of the same analyte. As a result, the Pade–Z would introduce multi-modality in the class-conditional distribution of each analyte. A second possibility would be to force the Pade–Z procedure to return a fixed number of exponentials or consider only those solutions that contain the desired number of exponentials. Our experience shows that this alternative produces solutions that are a poor fit to the experimental data.

In this article, we propose an elegant and efficient solution to yield a constant number of features regardless of the number of exponentials returned by the Pade–Z procedure. Our approach is based on the Taylor series expansion of the exponential function:

$$e^x = 1 + x + \frac{x^2}{2!} + \frac{x^3}{3!} + \dots = \sum_{n=0}^{\infty} \frac{x^n}{n!}. \quad (13)$$

Performing this expansion to each of the exponential decays in (1):

$$\sum_{m=1}^M G_m e^{-t/\tau_m} = \sum_{m=1}^M G_m \sum_{n=0}^{\infty} \frac{(-t/\tau_m)^n}{n!} = \sum_{n=0}^{\infty} \frac{(-t)^n}{n!} \sum_{m=1}^M \frac{G_m}{\tau_m^n}, \quad (14)$$

which yields any desired number of features:

$$\left\{ \sum_{m=1}^M G_m, \sum_{m=1}^M \frac{G_m}{\tau_m}, \sum_{m=1}^M \frac{G_m}{\tau_m^2}, \sum_{m=1}^M \frac{G_m}{\tau_m^3}, \dots \right\}. \quad (15)$$

The first feature, $\sum_{m=1}^M G_m$, has a simple interpretation as it is the steady-state response of the sensor. Subsequent features are a weighted sum of the amplitudes by increasing powers of their time constants. As a result, as $n \rightarrow \infty$, the faster exponential decays dominate the higher features in (15).

4. Performance measures

Two independent measures of performance, sensitivity and selectivity, are proposed in this article to establish the relative merits of the different transient analysis techniques. For the purpose of measuring sensitivity, we define a classification scenario where the goal is to estimate the identity and intensity of a given analyte from a set of P possible “primary” analytes, each of them having D different dilution levels. In this case, sensitivity can be simply measured by determining the recognition rate of a pattern classifier for different analyte concentrations. At relatively high concentrations (but below sensor saturation), the sensor-array response for different odors will be discriminative and repeatable, whereas at lower concentrations the responses become weaker and, therefore, more subject to interferences (i.e. temperature and drift). As a result, classification rates will be proportional to concentration, as illustrated in Fig. 5(a) for a hypothetical case where two potential transient analysis techniques are being evaluated. The most sensitive technique will be the one whose feature set produces higher classification rates at near-threshold concentrations. For the example illustrated in Fig. 5(a), this clearly corresponds to feature set 1. Misclassifications are penalized according to the following cost function:

$$\text{cost}(X_i|Y_j) = \frac{1}{\alpha} d(X, Y) + \frac{1}{\beta} d(i, j), \quad (16)$$

where X_i is a sample of analyte X at concentration i , Y_j a sample of analyte Y at concentration j , and $\text{cost}(X_i|Y_j)$ the cost of classifying Y_j as X_i . The first term in the summation penalizes misidentifying the analyte, regardless of concentration:

$$d(X, Y) = \begin{cases} 0, & X = Y, \\ 1, & X \neq Y, \end{cases} \quad (17)$$

whereas the second term applies a penalty that is proportional to the distance between the predicted and the true concentration of the analyte:

$$d(i, j) = |i - j|. \quad (18)$$

The terms α and β serve as normalizing constants to ensure that the cost is bounded [0, 1]. For the experiments described in Section 6.1, these constants were set to $\alpha = 2$ and $\beta = 5$.

response of each sensor. This feature vector is used to provide a reference performance level for the thermal transient feature sets.

- **WTS**: Four WTS kernels are used to extract information from the time domain transient, as illustrated in Fig. 3(a). Therefore, each analyte sample contains 4 features for each of the 6 sensor transients, for a total of 24 features per sensor.
- **Pade–Z**: Four features are extracted from the $\{\tau_m, G_m\}$ pairs returned by Pade–Z, as described by Eq. (15). Thus, each sample contains 24 features per sensor.
- **METS**: Four WTS kernels are used to extract information from the METS signal, as outlined in Fig. 3(b), for a total of 24 features per sensor.
- **RRCF**: Four WTS kernels are also used to extract information from the RRCF signal, as outlined in Fig. 3(b), for a total of 24 features per sensor.

6. Results

Two separate databases were collected over a period of 2 weeks to establish the sensitivity and selectivity of the above-mentioned feature sets. During the course of these experiments the third and fourth sensors in the array became faulty, and had to be discarded for the subsequent computational analyses. Therefore, each sample of an analyte consisted of 6 thermal transients for 2 sensors, for a total of 12 transients. The final dimensionality of the five feature sets is summarized in Table 1.

6.1. Sensitivity analysis

To establish the sensitivity improvements of the different techniques, a database of five serial dilutions in distilled water was collected on the sensor array. The highest concentration level of each analyte (acetone, 10^{-4} vol.%; isopropyl alcohol, 10^{-1} vol.%; ammonia, 1.0 vol.%) was selected three dilution factors above the isothermal detection threshold of the sensor array, defined as the concentration at which the average steady-state response across the sensors (with a constant 5 V heater voltage) could not discriminate the diluted analyte from distilled water. Lower concentrations of the analytes were obtained by serial dilution in

distilled water with a dilution factor of 10. Thus, these dilutions represent a dynamic range of five logarithmic units.

The dataset was collected over a period of 4 days. On each day, 15 samples were prepared, 5 dilutions for each of the 3 analytes. In addition, two water samples were collected each day, one at the beginning of the session and a second one at the end, to verify that the sensor patterns did not have trends as a result of heating. Classification was performed using the k nearest-neighbor classifier [32] with $k = 3$ neighbors. Classifier performance was estimated through four-fold cross-validation, where each fold was defined as the samples collected in a particular day. Thus, the classification measure also penalized transient analysis techniques that were sensitive to drift.

The resulting classification rate, as defined by Eq. (16), is illustrated in Fig. 6(a). RRCF provides the best performance, both overall and on each particular concentration. WTS, Pade–Z and METS achieve similar performance, whereas dc yields the poorest sensitivity. These results clearly indicate that the thermal transients contain additional information that can be used to improve the sensitivity of commercial metal-oxide sensors. We anticipate that improved performance may be achieved by placing the WTS kernels in those regions of the transient or spectrum that are known to contain more discriminatory information.

6.2. Selectivity analysis

To analyze the selectivity of these techniques, a second dataset was collected with the same sensor array and experimental protocol. In this case, the samples consisted of individual analytes, and their binary and ternary mixtures. The base concentration used for acetone, isopropyl alcohol and ammonia was 0.3, 1.0 and 33 vol.%, respectively. These concentrations were chosen so that they produced the same average response on the sensor array, preventing an individual analyte from dominating the mixtures.

Three individual analytes (A, I and M), three binary mixtures (AI, AM and IM), one ternary mixture (AIM) and distilled water (W) were used. Two serial dilutions with a dilution factor of 1/3 were also processed, for a total of 24 samples per day (7 mixtures \times 3 concentrations plus 3 water samples). The experiment was repeated three times on three consecutive days.

Classification performance was estimated using the $k = 3$ nearest-neighbor rule and three-fold cross-validation, where each fold represented the samples collected in a particular day. When the complete feature vector is used (see Table 1), the classification rate for dc, WTS, Pade–Z, METS and RRCF is 96, 96, 89, 94 and 93%, respectively. These results show that dc and WTS provide comparable selectivity, closely followed by the two spectral techniques. Pade–Z, however, falls short of the performance provided by dc.

To gain a better understanding of these results, we perform a principal components decomposition of each feature set and analyze the behavior of the selectivity measure as a

Table 1
Dimensionality of the feature sets under study

Feature set	Number of sensors	Number of transients per sensor	Number of features per transient	Total number of features
dc	2	6	1	12
WTS	2	6	4	48
Pade–Z	2	6	4	48
METS	2	6	4	48
RRCF	2	6	4	48

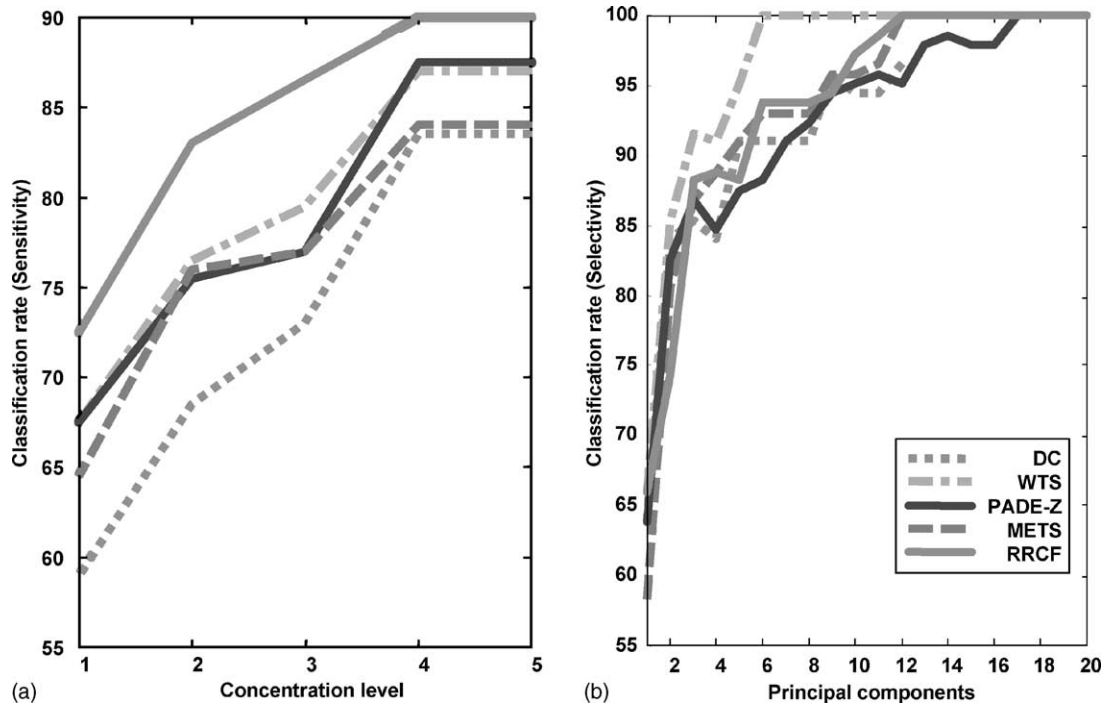


Fig. 6. Sensitivity (a) and selectivity (b) performance of the different feature sets.

function of the number of principal components used in the Ho-Kashyap regression. The results, illustrated in Fig. 6(b), allow us to make two interesting observations. First, improved performance can be achieved in most cases by preserving only the larger eigenvalues. This allows WTS and RRCF to achieve 100% selectivity, and significantly improve the performance of METS and Pade-Z. Pade-Z, however, is not able to outperform dc. A second conclusion can be extracted by observing that WTS reaches 100% classification rate with fewer principal components than any other technique, indicating that the WTS features are more highly correlated. This result should come at no surprise considering the monotonicity of the sensor transients. Two opposing arguments can be made about this result. On one hand, the more compact representation provided by WTS is clearly desirable as it reduces the complexity of a subsequent classifier. On the other hand, one may view the spectral techniques (METS and RRCF) as being able to provide features that are more “orthogonal”. In practice, either argument is likely to be overridden by the final performance on each particular sensor array and application.

7. Summary

This article has presented a temperature modulation procedure to improve the sensitivity and selectivity of commercial metal-oxide sensors. The sensors are driven by a staircase temperature profile, and the thermally-induced transients are used to extract additional information from the sensor. Four different transient analysis have been analyzed,

WTS, Pade-Z, METS and RRCF. WTS operates on the time domain, whereas the remaining techniques perform a spectral or time-constant analysis. Feature extraction procedures for each of these transient analysis techniques have also been discussed, along with two performance measures based on sensitivity and selectivity. For the purpose of measuring selectivity, a novel linear separability criterion has also been presented.

Experimental validation of our excitation and computational methods has been performed on a sensor array exposed to serial dilutions and mixtures of three analytes. A sensitivity analysis on serial dilutions near the isothermal detection threshold shows that the four transient analysis techniques outperform a feature vector consisting of quasi-stationary temperature-modulated responses. Our novel ridge regression curve fitting technique provides the best performance, both overall and at each particular concentration. Experiments on selectivity using binary and ternary mixtures at three concentration levels indicate that the principal components of three out of four transient analysis techniques provide better performance than quasi-stationary features. It is expected that improved performance may be obtained by proper selection of the position and width of the kernel windows used to extract features from the spectral signals [33].

Acknowledgements

This material is based upon work supported by the National Science Foundation under CAREER Grant No. 9984426/0229598.

References

- [1] A.P. Lee, B.J. Reedy, Temperature modulation in semiconductor gas sensing, *Sens. Actuators B* 60 (1999) 35–42.
- [2] R. Gutierrez-Osuna, S. Korah, A. Perera, in: *Proceedings of the Eighth International Symposium on Olfaction and Electronic Nose*, Washington, DC, 2001.
- [3] W.M. Sears, K. Colbow, F. Consadori, General characteristics of thermally cycled tin oxide gas sensors, *Semicond. Sci. Technol.* 4 (1989) 351–359.
- [4] W.M. Sears, K. Colbow, F. Consadori, Algorithms to improve the selectivity of thermally cycled tin oxide gas sensors, *Sens. Actuators B* 19 (1989) 333–349.
- [5] S. Nakata, Y. Kaneda, H. Nakamura, K. Yoshikawa, Detection and quantification of CO gas based on the dynamic response of a ceramic sensor, *Chem. Lett.* (1991) 1505–1508.
- [6] S. Nakata, H. Nakamura, K. Yoshikawa, New strategy for the development of a gas sensor based on the dynamic characteristics: principle and preliminary experiment, *Sens. Actuators B* 8 (1992) 187–189.
- [7] S. Nakata, S. Akakabe, M. Nakasuji, K. Yoshikawa, Gas sensing based on a non-linear response: discrimination between hydrocarbons and quantification of individual components in a gas mixture, *Anal. Chem.* 68 (1996) 2067–2072.
- [8] S. Nakata, K. Yoshikawa, Non-linear dynamics in chemical assembly, *Trends Chem. Phys.* 4 (1996) 23–58.
- [9] S. Nakata, E. Ozaki, N. Ojima, Gas sensing based on the dynamic non-linear responses of a semiconductor gas sensor: dependence on the range and frequency of a cyclic temperature change, *Anal. Chim. Acta* 361 (1998) 93–100.
- [10] A. Heilig, N. Barsan, U. Weimar, M. Schweizer-Berberich, J.W. Gardner, W. Gopel, Gas identification by modulating temperatures of SnO₂-based thick film sensors, *Sens. Actuators B* 43 (1997) 45–51.
- [11] E. Llobet, R. Ionescu, S. Al-Khalifa, J. Brezmes, X. Vilanova, X. Correig, N. Barsan, J.W. Gardner, Multi-component gas mixture analysis using a single tin oxide sensor and dynamic pattern recognition, *IEEE Sens. J.* 1 (3) (2001) 207–213.
- [12] M.O. Perez-Lisboa, M. Barriga-Puente de la Vega, F.J. Ramirez-Fernandez, Study of sensitivity and selectiveness of gas sensor array to periodic stimuli, in: *Proceedings of the International Conference on Microelectronics and Packaging (ICMP99)*, vol. 1, Campinas, SP, 1999, pp. 267–269.
- [13] S. Wlodek, K. Colbow, F. Consadori, Signal-shape analysis of a thermally cycled tin oxide gas sensor, *Sens. Actuators B* 3 (1991) 63–68.
- [14] T.A. Kunt, Dynamic modelling and optimization of micro-hotplate chemical gas sensors, Ph.D. dissertation, University of Maryland, College Park, MD, 1997.
- [15] T.A. Kunt, T.J. McAvoy, R.E. Cavicchi, S. Semancik, Optimization of temperature programmed sensing for gas identification using micro-hotplate sensors, *Sens. Actuators B* 53 (1998) 24–43.
- [16] Y. Hiranaka, T. Abe, H. Murata, Gas-dependent response in the temperature transient of SnO₂ gas sensors, *Sens. Actuators B* 9 (1992) 177–182.
- [17] T. Amamoto, T. Yamaguchi, Y. Matsuura, Y. Kajiyama, Development of pulse drive semiconductor gas sensor, *Sens. Actuators B* 13–14 (1993) 587–588.
- [18] Y. Kato, K. Yoshikawa, M. Kitora, Temperature-dependent dynamic response enables the qualification and quantification of gases by a single sensor, *Sens. Actuators B* 40 (1997) 33–37.
- [19] B. Yea, T. Osaki, K. Sugahara, R. Konishi, The concentration-estimation of inflammable gases with a semiconductor gas sensor utilizing neural networks and fuzzy inference, *Sens. Actuators B* 41 (1997) 121–129.
- [20] Figaro 1996, Figaro Engineering Inc., Osaka, Japan.
- [21] R. Gutierrez-Osuna, H.T. Nagle, S.S. Schiffman, Transient response analysis of an electronic nose using multi-exponential models, *Sens. Actuators B* 61 (1–3) (1999) 170–182.
- [22] E. Yeramian, P. Claverie, Analysis of multi-exponential functions without a hypothesis as to the number of components, *Nature* 326 (1987) 169–174.
- [23] S. Marco, J. Samitier, J.R. Morante, A novel time domain method to analyze multi-component exponential transients, *Meas. Sci. Technol.* 6 (1995) 135–142.
- [24] B.G. Kermani, On using neural networks and genetic algorithms to optimize the performance of an electronic nose, Ph.D. dissertation, North Carolina State University, Raleigh, NC, 1995.
- [25] C. Lanczos, *Applied Analysis*, Prentice-Hall, Englewood Cliffs, NJ, 1956.
- [26] D.G. Gardner, J.C. Gardner, G.L. Laush, W.W. Meinke, Method for the analysis of multi-component exponential decay curves, *J. Chem. Phys.* 31 (1959) 978–986.
- [27] L. Weiss, R.N. McDonough, Prony's method, Z-transforms, and Pade approximation, *SIAM Rev.* 5 (2) (1963) 145–149.
- [28] C.L. Phillips, H.T. Nagle, *Digital Control Systems Analysis and Design*, Prentice-Hall, Englewood Cliffs, 1995.
- [29] R. Gutierrez-Osuna, Signal processing and pattern recognition for an electronic nose, Ph.D. dissertation, North Carolina State University, Raleigh, NC, 1998.
- [30] R. Gutierrez-Osuna, Pattern analysis for machine olfaction: a review, *IEEE Sens. J.* 2 (3) (2002) 189–202.
- [31] R. Gutierrez-Osuna, H.T. Nagle, B. Kermani, S.S. Schiffman, Signal conditioning and preprocessing, in: T.C. Pearce, S.S. Schiffman, H.T. Nagle, J.W. Gardner (Eds.), *Handbook of Machine Olfaction: Electronic Nose Technology*, Wiley-VCH, New York, 2002.
- [32] R.O. Duda, P.E. Hart, D.G. Stork, *Pattern Classification*, Wiley, New York, 2001.
- [33] D.E. Courte, M.A. Rizki, L.A. Tamburino, R. Gutierrez-Osuna, Evolutionary optimization of Gaussian windowing functions for data preprocessing, *Int. J. Artif. Intell. Tools* 12 (1) (2003).

Biographies

Ricardo Gutierrez-Osuna received his BS degree in industrial/electronics engineering from the Polytechnic University of Madrid in 1992, and MS and PhD degrees in computer engineering from North Carolina State University in 1995 and 1998, respectively. From 1998 to 2002, he served the Faculty at Wright State University. He is currently an assistant professor in the Department of Computer Science at Texas A&M University. His research interests include pattern recognition, machine learning, biological cybernetics, machine olfaction, speech-driven facial animation, computer vision and mobile robotics.

Agustin Gutierrez-Galvez received his BS in physics and BS in electrical engineering in 1995 and 2000, respectively, both from the Universitat de Barcelona. He is currently pursuing his PhD degree in computer engineering at Texas A&M University. His research interests are neuro-morphic models of the olfactory system and pattern recognition applied to odor detection with sensor arrays.

Nilesh Powar obtained his BS in electronics engineering from the University of Bombay, India, in 1999. He is currently pursuing his MS degree in computer engineering at Wright State University. His research interests include pattern recognition, bioinformatics, sensor systems, systems programming and concurrent software systems.